JOURNAL OF MATERIALS SCIENCE 29 (1994) 1818–1824

Corrosion behaviour of TiN films obtained by plasma-assisted chemical vapour deposition

C. B. IN, S. P. KIM, J. S. CHUN
Department of Electronic Materials Engineering, Korea Advanced Institute of Science and Technology, 373-1 Kusong Dong, Yusong Gu, Taejon, South Korea

Titanium nitride (TiN) coatings with a dense structure were prepared on high-speed steel by plasma-assisted chemical vapour deposition (PACVD). The electrochemical polarization measurement of TiN coating was compared with that of the uncoated substrate. It was found that the TiN coating had a higher corrosion potential, and a lower corrosion rate (current density), about three orders of magnitude less than for the steel substrate. The major corrosion mechanism of TiN was pitting corrosion through surface defects and/or open pores. The number and size of pits decreased with the chlorine content of the film. The TiN coating deposited by PACVD, regardless of the amount of residual chlorine, proved to be a good anti-corrosion coating on a steel substrate.

1. Introduction

TiN has good electrical and mechanical properties in addition to corrosion resistance, because of its low reactivity with the environment [1–4]. MCrAlY coating (where M can be Fe, Co etc.), which is used as an anti-oxidation coating for the turbine blades of aircraft engines, shows deterioration of the oxidation resistance property at elevated temperature through interdiffusion between the coating and the Ni-based superalloy substrate to form NiAl alloy. Research to prevent this phenomenon has been in progress and Coad *et al.* [5] reported good anti-oxidation properties using TiN as a diffusion barrier, which has good chemical stability and good compatibility with the two materials.

TiN, TiC and Ti(CN) films prepared by chemical vapour deposition (CVD) [6–8] have been reported to have better adhesion properties with the substrate than those prepared by physical vapour deposition (PVD) [9, 10]. However, for coating steel tools, the high-temperature processes involved (usually above 1000 °C) can degrade the mechanical properties of the substrate. Over the past few years there have been researches on plasma-assisted CVD (PACVD) of TiN on steel [11–17], as this is expected to deposit a more uniform coating on complex-shaped surfaces at low temperature. Recently, Li Shizhi *et al.* [14] reported that TiN and Ti(CN) were deposited on to steel tools with a pilot production-scale PACVD apparatus.

TiN is a chemically very stable coating for many steels in most environments, but pores or pinholes in the coating may accelerate corrosion by certain corrosion mechanisms. Since TiN is an electrical conductor and electrochemically nobler than steel, open pores in the coating can act as a small anode area which accelerates the corrosion. Also many surface defects in the coating may deteriorate the protective ability.

In analysing defect effects, the electrochemical method offers information on the microscopic structure such as the amount and distribution of open pores in the coating, in addition to other defect structures, which cannot be acquired by means of scanning electron microscopy (SEM) and transmission electron microscopy (TEM).

In this study we have used the electrochemical polarization method to determine the corrosion behaviour and the corrosion mechanism of TiN deposited on to steel by PACVD.

2. Experimental procedure

2.1. Deposition

TiN was deposited on to high-speed steel (AISI M2, 1.2 cm × 1.8 cm × 0.3 cm) with 63 ± 1 HRC (Rockwell Hardness Value) by PACVD using a gaseous mixture of $TiCl_4$, N_2, H_2 and Ar. A schematic diagram of the apparatus is shown in Fig. 1. The detailed deposition procedure is described elsewhere [15–17]. Before deposition the surface of the substrate was mechanically polished using 220, 400, 800 and 1500 grit SiC papers. Subsequently it was polished using a 1 μm alumina paste on cloth, and finally acetone cleaning was performed with an ultrasonic cleaner. The variable of the deposition conditions was substrate temperature, from 450 to 550 °C, and other deposition parameters were fixed as follows: deposition pressure 3 torr, total flow rate 200 sccm ($TiCl_4$ 2 sccm, N_2 70 sccm, H_2 40 sccm, Ar 88 sccm), r.f. power 45 W, interelectrode distance 5 cm.

2.2. Measurements

The surface morphology and fractured cross-section of TiN were observed by SEM and the microstructure and grain size were observed by TEM. The analysis of

0022–2461

chlorine content was carried out with Auger electron spectroscopy (AES) (Perkin-Elmer SAM 4300), applying 3 keV, 0.8 μA Ar ion with the incident angle of electron beam at 30°

The electrochemical measurement was done with a microcomputer-controlled potentiostat (EG&G M 273) by measuring the cyclic polarization. The measurement was carried out in an electrolyte of 0.01 N HCl with pH 2, and the area exposed to HCl solution was 1 cm^2. The sweep rate of potential was 0.5 $mV\,s^{-1}$ and the test temperature was 20 °C. Generally, since the surface of the sample was somewhat oxidized, the sample was cathodically reduced at − 500 mV (with respect to a saturated calomel electrode (SCE)) for 5 min at the beginning of the each test. After a potential sweep to the positive direction from − 500 mV to 1500 mV, the scan direction was reversed to the negative direction to 1200 mV.

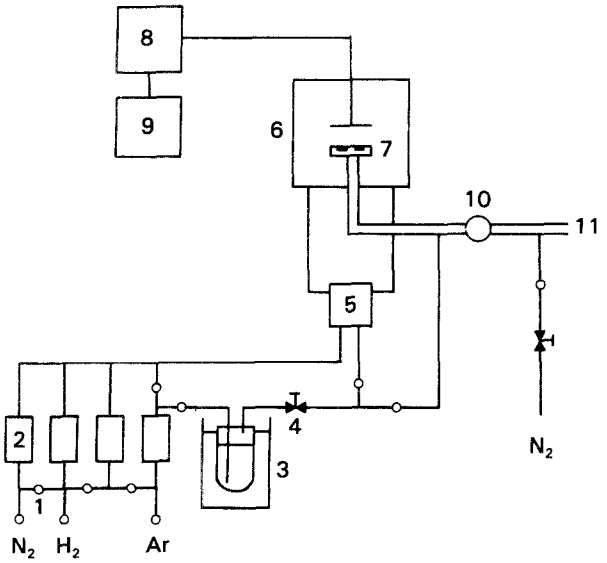

Figure 1 Schematic diagram of experimental apparatus for PACVD of TiN (1) air-operated bellows valve, (2) mass flow controller, (3) $TiCl_4$ bubbler, (4) fine metering valve, (5) gas mixing box, (6) vacuum chamber, (7) heater, (8) automatic matching network, (9) r.f. generator, (10) plug valve, (11) vacuum system.

3. Results and discussion

3.1. Microscopic structure and compositional analysis

The typical surface morphology and fractured cross-section of TiN deposited by PACVD are shown in the SEM pictures of Fig. 2. TiN coating has a smooth and dense columnar structure. In order to examine the grain size and microstructure TEM was utilized. Fig. 3 shows selected-area diffraction patterns (SADPs) of films with different deposition temperatures of 450 and 550 °C. At the deposition temperature of 450 °C the grain size was about 10 nm (Fig. 3b). TiN deposited the 550 °C had a grain size of 20–50 nm (Fig. 3d). As the deposition temperature increases, the grain size increases due to the increase in the energy of reactive species and the difference of diffusion rates.

Fig. 4 shows the AES spectra of TiN coatings. Fig. 4a and c are the spectra of the as-received specimens, and show carbon and oxygen contamination at the surface which was most likely to have occurred during the transport of samples from the PACVD chamber to the AES chamber. After 4 min sputter-etching with an Ar ion beam, the spectra obtained are as represented in Fig. 4b and d. The composition of the TiN was analysed quantitatively according to Hofmann's method [18]. From this method, it was found that the TiN had an almost constant atomic ratio of N/Ti for the two different deposition temperatures, but the chlorine content varied largely from 20 at % for 450 °C to 5 at % for 550 °C. This result means that

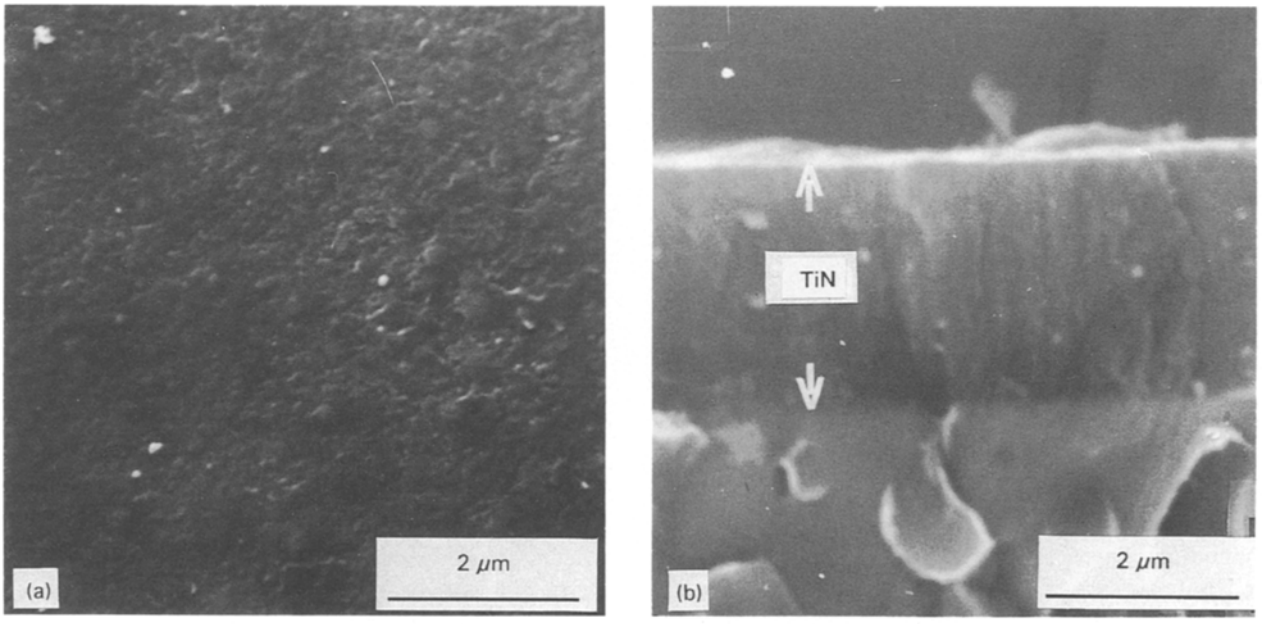

Figure 2 Typical SEM photographs of TiN deposited by PACVD: (a) surface morphology, (b) fractured cross-section.

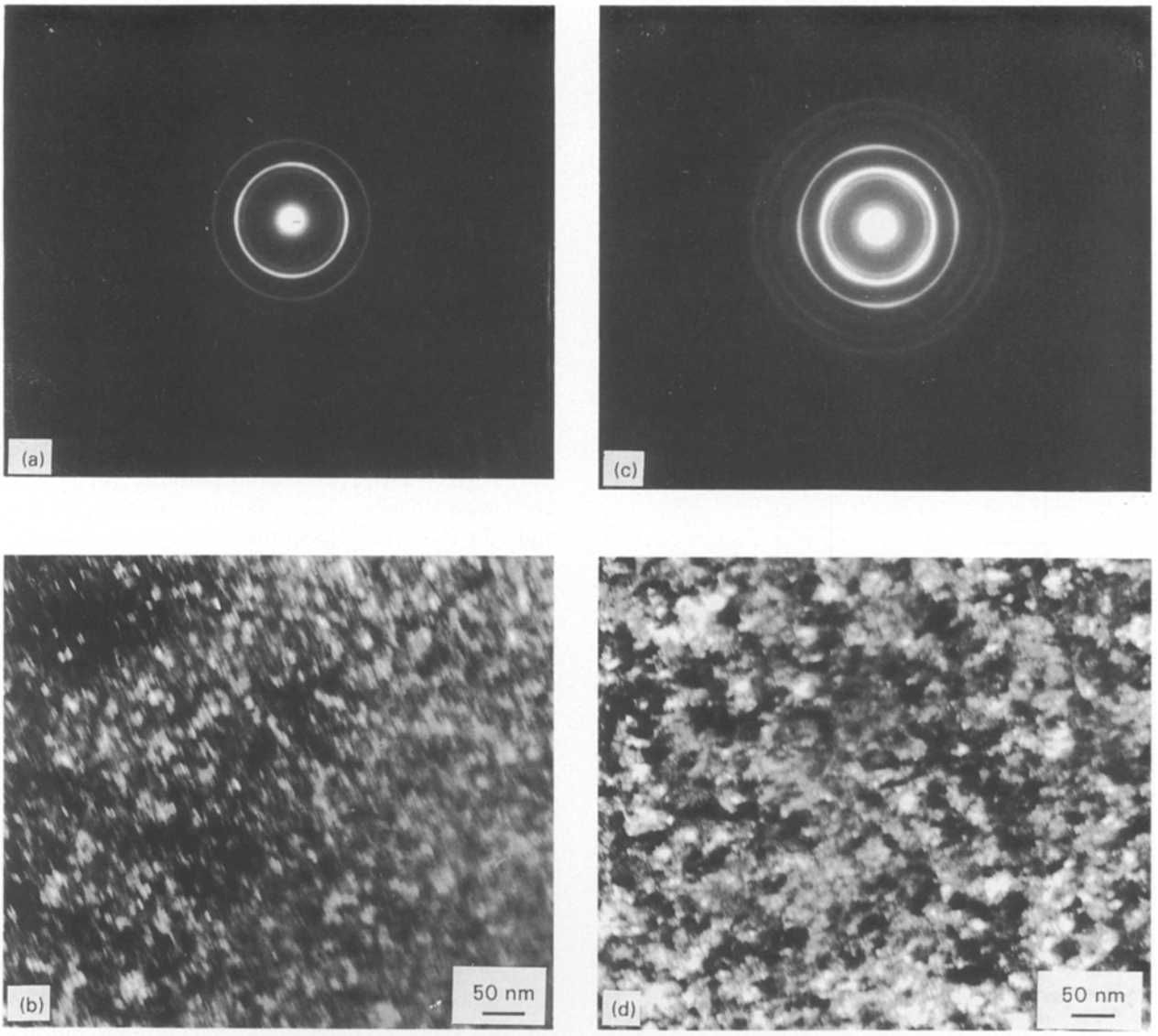

Figure 3 Selected-area diffraction patterns and transmission electron micrographs (dark-field images) of TiN films at different deposition temperatures: (a, b) 450 °C, (c, d) 550 °C.

the TiN deposition reaction and the desorption reaction of $TiCl_x(N)$ to Cl or HCl were kinetically enhanced with increase of temperature [16].

3.2. Electrochemical measurements

Fig. 5 and Table I show the results of the cyclic polarization measurements. The thickness of TiN for the tests was 0.5 μm. The corrosion potential of the M2 substrate was − 432 mV and those of the samples with deposition temperatures of 450 and 550 °C were − 304 and − 120 mV, respectively. The sample with TiN coating had a better corrosion resistance because of its higher corrosion potential than that of the substrate. The current density of the sample with TiN coating in the anodic area was about three orders of magnitude lower than the value for the uncoated substrate (i.e. 1×10^{-5} mA cm^{-2} for the sample with TiN coating and 8×10^{-3} mA cm^{-2} for the substrate sample).

TABLE I Result of polarization tests of Fig. 5

Sample	Corrosion potential (mV)	Corrosion current density (mA cm^{-2})
Substrate (M2)	− 432	2×10^{-2}
TiN deposited at 450 °C	− 304	5×10^{-3}
TiN deposited at 550 °C	− 120	1×10^{-5}

The surfaces of the samples were observed by SEM after the corrosion test and the pictures are shown in Figs 6 to 8. As a result of the polarization test of the uncoated substrate, general corrosion throughout the tested area with several pits occurred (Fig. 6). In contrast, the sample with TiN coatings had several pits without any general corrosion. By comparing Figs 7 and 8 it can be seen that the sample with TiN deposited at 450 °C had more large pits per unit area than that with TiN deposited at 550 °C. It is thought

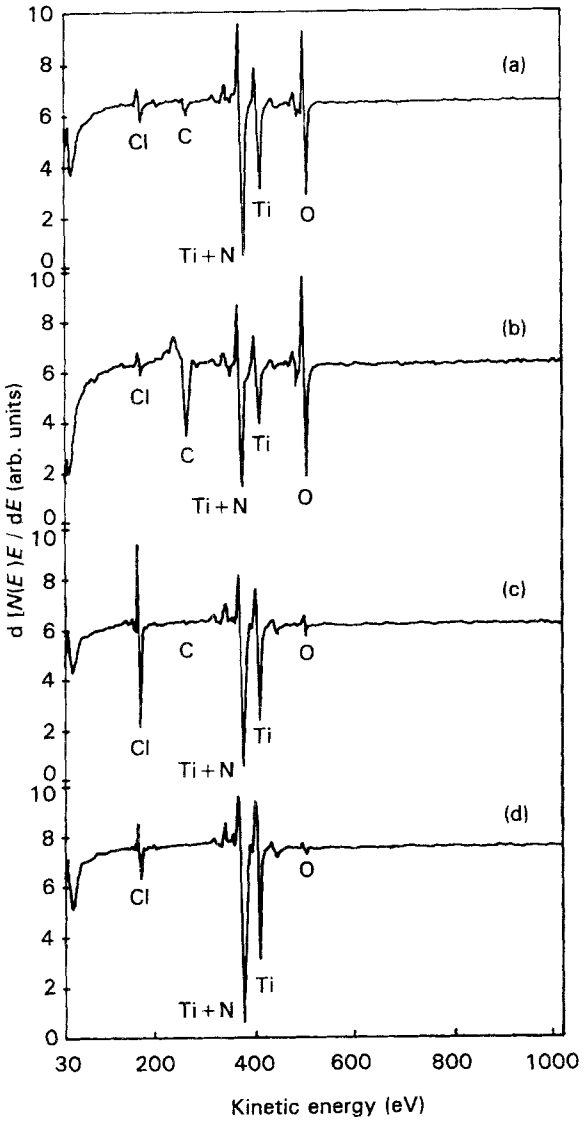

Figure 4 AES spectra of TiN films at different deposition temperatures: (a) as-received TiN film deposited at 450 °C, (b) as-received TiN film deposited at 550 °C, (c) after 4 min sputter-cleaning of TiN film deposited at 450 °C, (d) after 4 min sputter-cleaning of TiN film deposited at 550 °C.

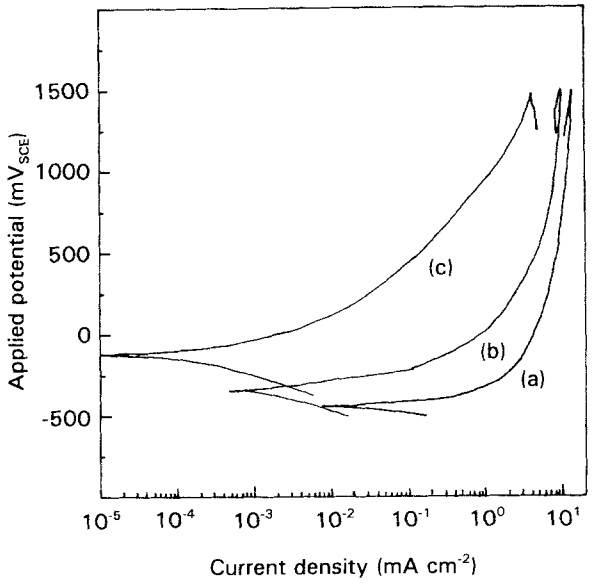

Figure 5 Potentiodynamic polarization curves: (a) substrate material, (b) sample with TiN deposited at 450 °C, (c) sample with TiN deposited at 550 °C.

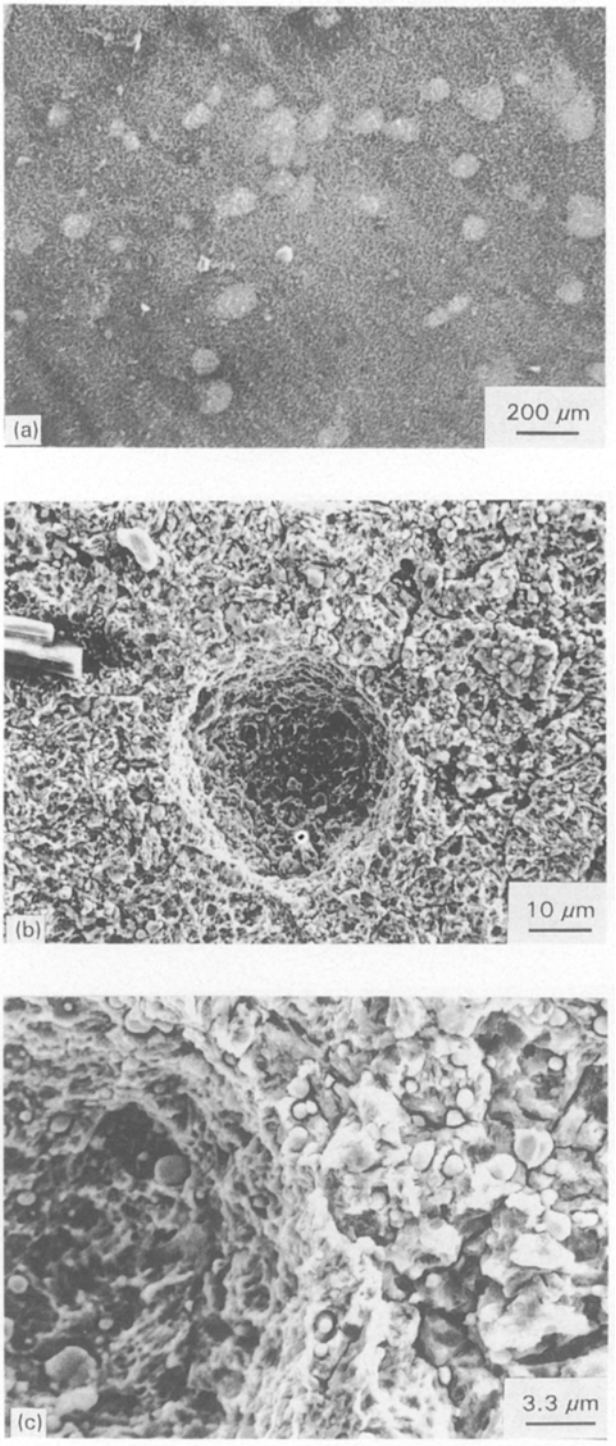

Figure 6 Surface mophology of substrate material after corrosion test: (a) corrosion area, (b) a corrosion pit, (c) inside corrosion pit.

that this result is related to the chlorine content in the coating as follows: since TiN with a large content of chlorine (i) had many open pores, with many corrosion pits appearing, and (ii) had a faster corrosion rate due to its less dense structure, the size of corrosion pits was greater than for TiN with a low content of chlorine.

Fig. 9 shows AES profiles of the sample with TiN deposited at 550 °C after the corrosion test. When the profile before the test (Fig. 4d) was compared with that of the flat area (undamaged area) after the test (Fig. 9a), the profiles were found to be almost the same.

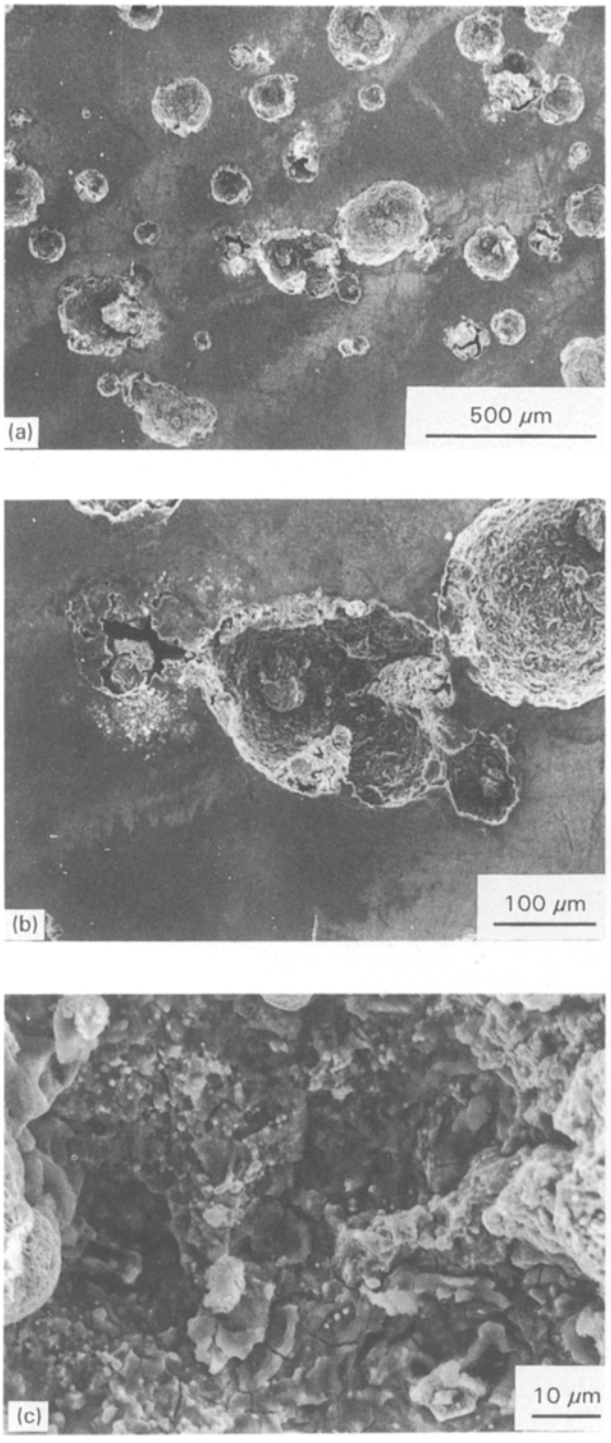

Figure 7 Surface mophology of sample with TiN deposited at 450 °C after corrosion test: (a) corrosion area, (b) corrosion pits, (c) inside corrosion pit.

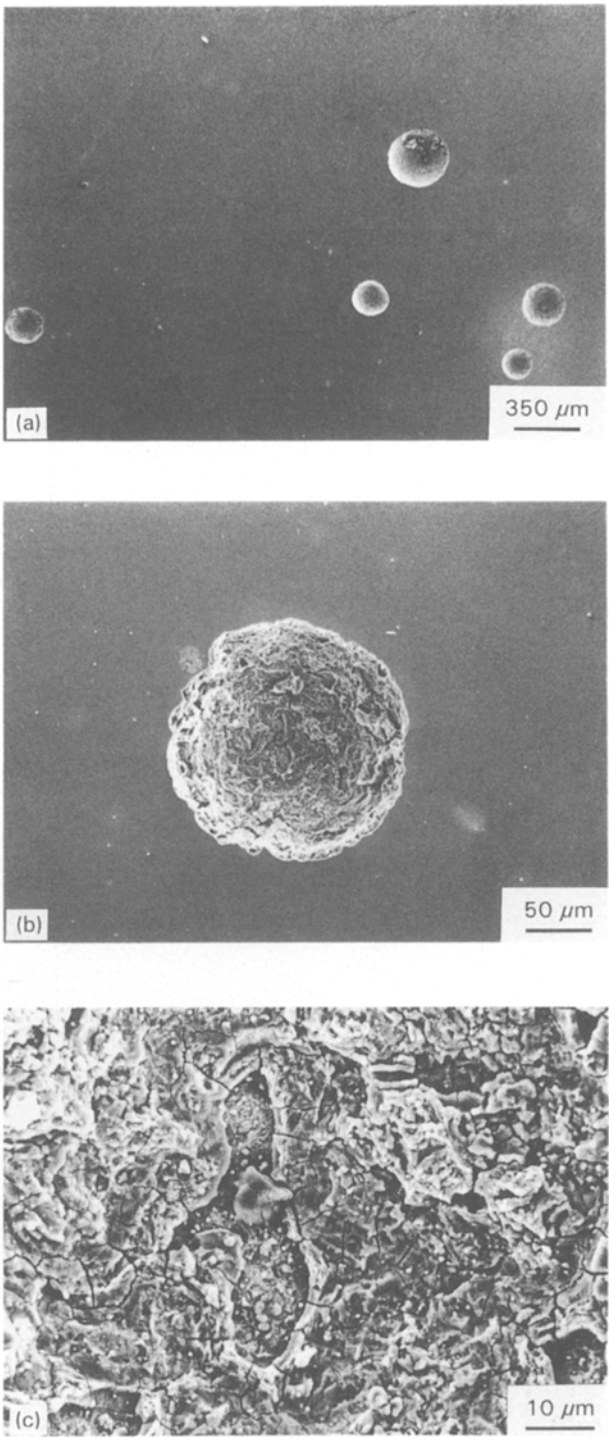

Figure 8 Surface mophology of sample with TiN deposited at 550 °C after corrosion test: (a) corrosion area, (b) a corrosion pit, (c) inside corrosion pit.

Thus craters (corrosion pits) occurred after the test through pitting corrosion at pores. From Fig. 9a, the other area (flat area) beside the pits seems to be undamaged and this result agrees with the former polarization test of Fig. 5. The AES profile of the crater area (Fig. 9b) showed a large amount of oxygen and chlorine, and no Ti and N spectra appeared. We think that the Cl peak of Fig. 9b comes from the HCl solution.

Fig. 10 shows an SEM photograph of a corrosion pit, demostrating the corrosion mechanism. The area marked A in Fig. 10 shows pieces of TiN isolated by pitting corrosion at surface defects and open pores. The isolated pieces of TiN are not thought to dissolve in the HCl solution. The SEM pictures in Fig. 11 show selected regions in one specimen with TiN film deposited at 450 °C, and are thought to show the developing steps of TiN pit formation which explain the proposed theory of corrosion mechanism in Fig. 12. Fig. 11a shows the separation of the TiN film into small pieces and general corrosion of the M2 substrate, and Fig. 12b, c and d are sequential steps following Fig. 12a.

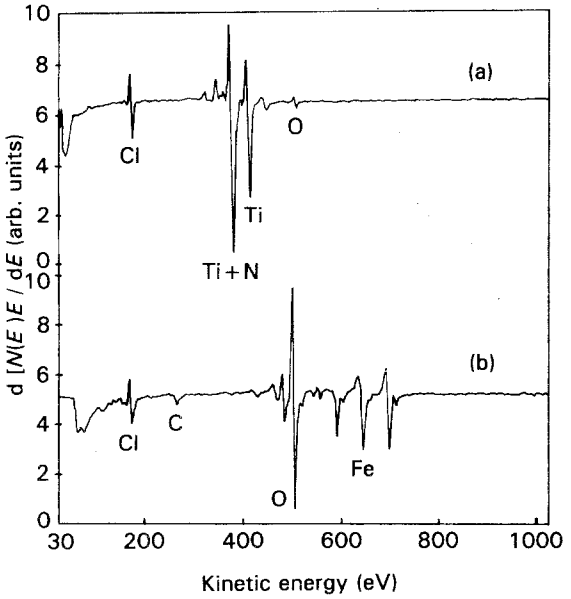

Figure 9 AES spectra of sample with TiN deposited at 550 °C after corrosion test: (a) flat area (undamaged area), (b) crater area (corrosion pit).

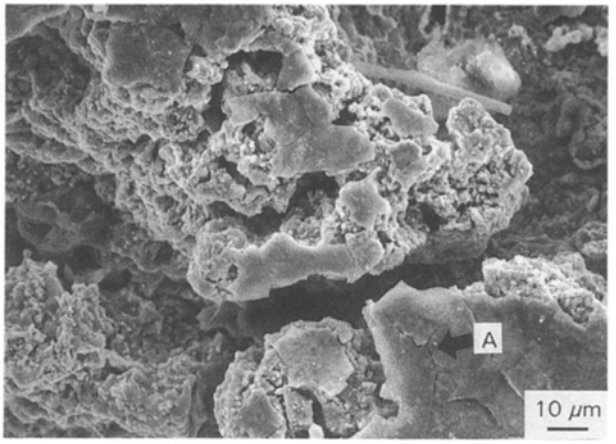

Figure 10 SEM photograph of corrosion pit demonstrating the corrosion mechanism.

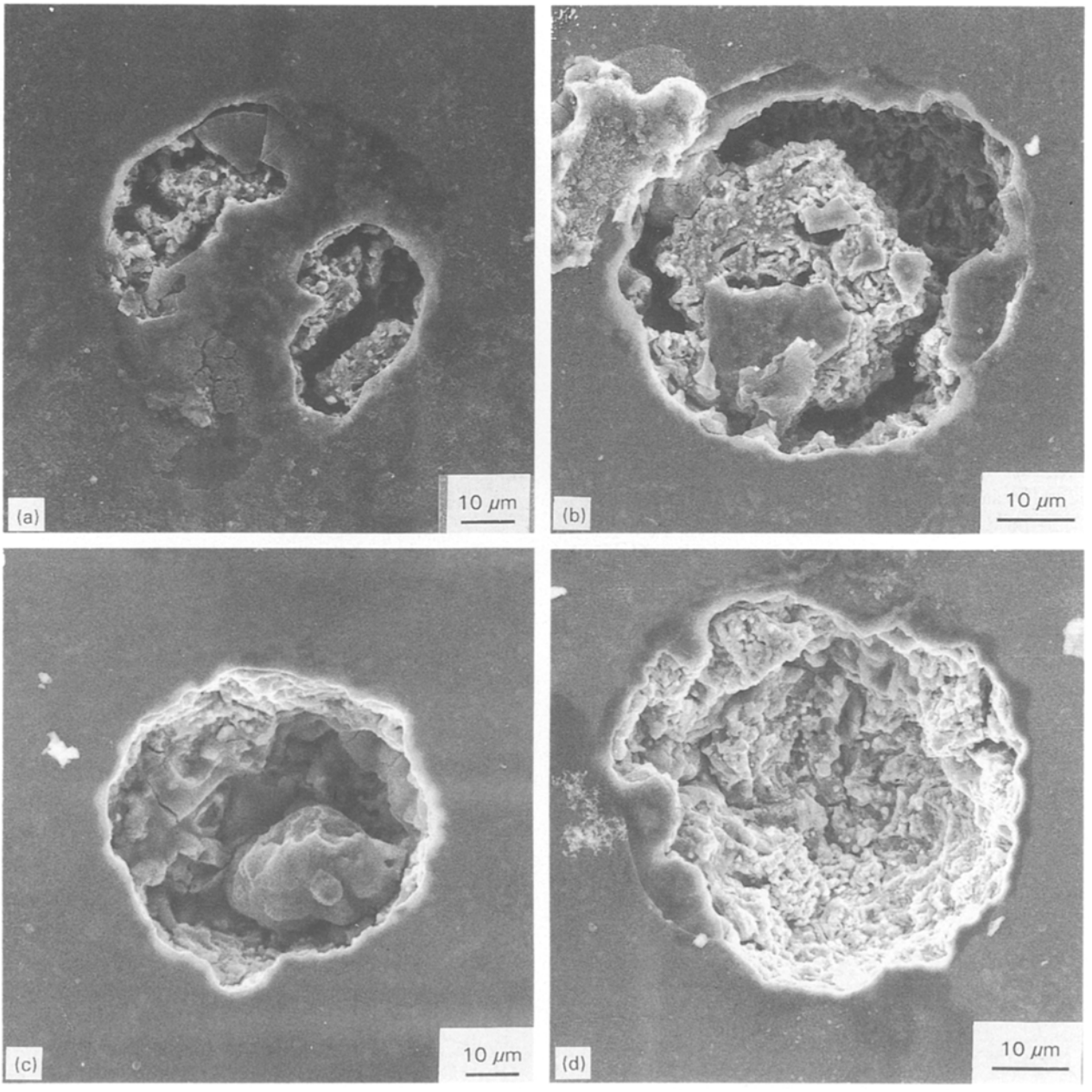

Figure 11 SEM photographs showing the advancing steps of crater formation.

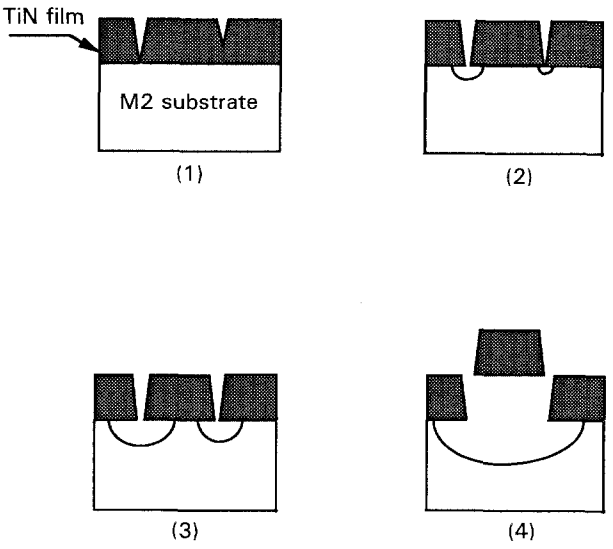

Figure 12 Schematic diagram of steps in the corrosion mechanism of TiN film: (1) pitting corrosion of TiN film through surface defects and open pores, (2) exposure of M2 substrate to electrolyte, (3) general corrosion of M2 substrate, (4) separation of corroded piece of TiN film.

The general corrosion of substrate around the centre left an isolated island with a small TiN film fragment (Fig. 12b); then as the corrosion advanced, the TiN film got separated and corrosion of the island occurred rapidly (Fig. 12c). Finally the island of substrate disappeared and a whole round pit had formed (Fig. 12d); advance of the crater's edge can be seen by signs of collapse of the TiN film.

By analysing Figs 10 and 11, we think that the corrosion mechanism of TiN coating may be concluded to consist of three stages. First, pitting corrosion occurs at the open pores and defects of the surface, and propagates to the interface area between the two materials. Second, general corrosion of the M2 substrate exposed to aqueous solution occurs, and finally, separation of the corroded TiN piece occurs. The modelling of this mechanism is shown in Fig. 12. From the results of polarization curves, SEM and AES data, it can be concluded that the TiN film acts as a good anti-corrosion coating when deposited on to a steel surface.

4. Conclusion

TiN coatings with a smooth and dense columnar structure were prepared by PACVD. The corrosion potential of the M2 substrate was -432 mV and that of the sample with TiN was -120 mV. The current density in the anode area of the sample with TiN coating was about three orders of magnitude lower than the value for the substrate. As residual chlorine in the coating increased, the corrosion rate increased. It is thought that the residual chlorine induces some kinds of lattice imperfection. Despite this phenomenon, it is thought that TiN film deposited on to a steel surface by PACVD is a good anti-corrosion coating. The corrosion mechanism of TiN coating is revealed to consist of three stages as follows: (i) initiation of pitting corrosion at the open pores and defects of the surface, with propagation to the interface area between the two materials; (ii) general corrosion of the M2 substrate exposed to aqueous solution; and (iii) separation of corroded TiN film fragments.

References

1. S. MASSIANI, A. MEDJAHED, P. GRAVIER, L. ARGEME and L. FEDRIZZI, *Thin Solid Films* **191** (1990) 305.
2. A. ERDEMIR, W. B. CARTER, R. F. HOCHMAN and E. I. MELETIS, *Mater. Sci. Eng.* **69** (1985) 89.
3. T. A. MÄNTYLÄ, P. J. HELEVIRTA, T. T. LEPISTÖ and P. T. SIITONEN, *Thin Solid Films* **126** (1985) 275.
4. M. J. PARK, A. LEYLAND and A. MATTHEWS, *Surf. Coat. Technol.* **43/44** (1990) 481.
5. J. P. COAD, D. S. RICKERBY and B. C. OBERLANDER, *Mater. Sci. Eng.* **174** (1985) 93.
6. A. J. PERRY and E. HORVATH, *Thin Solid Films* **62** (1979) 133.
7. D. G. BHAT, T. CHO and P. T. WOERNER, *J. Vac. Sci. Technol.* **A4** (1986) 2713.
8. C. J. KANG, D. W. KIM, C. O. PARK and J. S. CHUN, *Mater. Manuf. Processes* **5** (1990) 63.
9. B. E. JACOBSON, R. NIMMAGADDA and R. F. BUNSHAR, *Thin Solid Films* **63** (1979) 333.
10. R. BUHL, H. K. PULKER and E. MOLL, *ibid.* **80** (1981) 265.
11. LI SHIZHI, HUANG WU, YANG HONGSHUN and WANG ZHONGSHU, *Plasma Chem. Plasma Process* **4** (1984) 147.
12. T. ARAI, H. FUJITA and K. OGURI, *Thin Solid Films* **165** (1988) 139.
13. N. KIKUCHI, Y. OOSAWA and A. NISHYAMA, in Proceedings of 9th International Conference on CVD. Pittsburgh, May 1984, edited by McD. Robinson, C. H. J. van den Brekel, G. W. Cullen and J. M. Blocher Jr. (Electrochemical Society, Pennington, 1984) p. 728.
14. LI SHIZHI, ZHAO CHENG, XU XIANG, SHI YULONG, YANG HONGSHUN, *Surf. Coat. Technol.* **43/44** (1990) 1007.
15. D. H. JANG, S. S. CHUN and J. G. KIM, *Thin Solid Films* **169** (1989) 57.
16. S. B. KIM, S. K. CHOI, J. S. CHUN and K. H. KIM, *J. Vac. Sci. Technol.* **A9** (1991) 2174.
17. D. H. JANG and J. S. CHUN, *ibid.* **A7** (1989) 31.
18. S. HOFMANN, *ibid.* **A4** (1986) 2789.

Received 27 January
and accepted 15 September 1993